THERMO-MICROPOLAR FLUID FLOW ALONG A VERTICAL PERMEABLE PLATE WITH UNIFORM SURFACE HEAT FLUX IN THE PRESENCE OF HEAT GENERATION

by

Mohammad M. RAHMAN, Ibrahim A. ELTAYEB, and Sheikh Mohammad M. RAHMAN

Original scientific paper
UDC: 532.543.5:536.628:66.011
BIBLID: 0354-9836, *13* (2009), 1, 23-36
DOI: 10.2298/TSCI0901023R

A two-dimensional steady convective flow of thermo-micropolar fluid past a vertical permeable flat plate in the presence of heat generation with uniform surface heat flux has been analyzed numerically. The local similarity solutions for the flow, microrotation (angular velocity) and heat transfer characteristics are illustrated graphically for various material parameters entering into the problem. The effects of the pertinent parameters on the local skin friction coefficient, plate couple stress, and the rate of heat transfer are also calculated and displayed graphically. The results show that skin friction coefficient (viscous drag) and the rate of heat transfer (Nusselt number) in micropolar fluid are less compared to that of the Newtonian fluid.

Key words: *micropolar fluid, convection, heat flux, heat generation, suction, self similar solution*

Introduction

A micropolar fluid is the fluid with internal structures in which coupling between the spin of each particle and the macroscopic velocity field is taken into account. The classical theories of continuum mechanics are inadequate to explicit the microscopic manifestations of such complex hydrodynamic behavior. The dynamics of micropolar fluids, originated from the theory of Eringen [1] has been a popular area of research for the last few decades as this class of fluids represents mathematically many industrially important fluids that may be applied to explain the flow of colloidal suspensions (Hadimoto *et al.* [2]), liquid crystals (Lockwood *et al*. [3]), polymeric fluids, human and animal blood (Ariman *et al.* [4]), body fluids and many other situations.

Ahmadi [5] presented solutions for the flow of a micropolar fluid past a semi-infinite plate taking into account micro-inertia effects using a Runge-Kutta shooting method with Newtonian iteration. Soundalgekar *et al*. [6] studied the flow and heat transfer past a continuously moving plate in a micropolar fluid. Gorla [7] studied mixed convection in a micropolar fluid from a vertical surface with uniform heat flux. Rees *et al.* [8] studied free convection boundary layer flow of micropolar fluids from a vertical flat plate while Mohammadein *et al.* [9] studied the same flow bounded by stretching sheet with prescribed wall heat flux, viscous dissipation and internal heat generation. Aissa *et al.* [10] studied joule heating effects on a micropolar fluid past a stretching sheet with variable electric conductivity. Markin *et al.* [11] obtained similarity solutions for the mixed convection flow over a vertical plate for the case of constant heat flux condition at the wall. Char *et al.* [12] have studied laminar free convection flow of micropolar fluids from a curved surface using cubic spline collocation method. Kelson *et al.* [13] studied micropolar fluid flow over a porous stretching sheet with strong suction or injection while Bhargava *et al*. [14] studied the same flow for mixed convection investigating the effects of surface boundary conditions. Recently, Bhargava *et al.* [15] also studied the above problem over a nonlinear stretching sheet.

The study of heat generation or absorption in moving fluids is important in problems dealing with chemical reactions and those concerned with dissociating fluids. Possible heat generation effects may alter the temperature distribution; consequently, the particle deposition rate in nuclear reactors, electronic chips and semi conductor wafers. Rahman *et al.* [16] studied magnetohydrodynamic convective flow of a micropolar fluid past a vertical porous plate in the presence of heat generation-absorption. Very recently Rahman *et al.* [17] studied radiative heat transfer flow of micropolar fluid along a porous plate immersed in a porous medium.

In the present study, we have extended the work of Rahman *et al.* [16] for free-forced convection and investigate the heat transfer characteristics of micropolar fluid compared to the Newtonian fluid along a heated vertical porous flat plate with variable suction and uniform surface heat flux in the presence of heat generation. The similarity solutions are then obtained numerically for various parameters entering into the problem using shooting method and discussed the results from the physical point of view.

Mathematical formulation

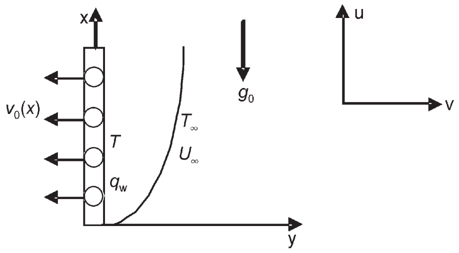

Figure 1. Flow configuration and coordinate system

Let us consider a steady two-dimensional flow of a viscous, incompressible micropolar fluid of temperature T_∞ past a heated vertical porous flat plate and there is a suction velocity $v_0(x)$ normal to the plate. The flow is assumed to be in the x-direction, which is taken along the plate in the upward direction and y-axis is normal to it. The flow configuration and the coordinate system are shown in the fig. 1.

Assuming the viscous dissipation effects to be negligible, the governing equations continuity, momentum, angular momentum and heat under Boussinesq and boundary layer approximation are as follows:

$$\frac{\partial u}{\partial x} \quad \frac{\partial v}{\partial y} \quad 0 \tag{1}$$

$$u\frac{\partial u}{\partial x} \quad v\frac{\partial u}{\partial y} \quad \upsilon \quad \frac{S}{\rho} \quad \frac{\partial^2 u}{\partial y^2} \quad \frac{S}{\rho}\frac{\partial \sigma}{\partial y} \quad g_0\beta^*(T \quad T_\infty) \tag{2}$$

$$u\frac{\partial \sigma}{\partial x} \quad v\frac{\partial \sigma}{\partial y} \quad \frac{\upsilon_s}{\rho j}\frac{\partial^2 \sigma}{\partial y^2} \quad \frac{S}{\rho j} \quad 2\sigma \quad \frac{\partial u}{\partial y} \tag{3}$$

$$u\frac{\partial T}{\partial x} \quad v\frac{\partial T}{\partial y} \quad \frac{\kappa}{\rho c_p}\frac{\partial^2 T}{\partial y^2} \quad \frac{Q_0}{\rho c_p}(T \quad T_\infty) \tag{4}$$

where u and v are the velocity components along x and y co-ordinates, respectively, $\upsilon = \mu/\rho$ is the kinematic viscosity, ρ – the mass density of the fluid, μ – the coefficient of dynamic viscosity, S – the coefficient of gyro-viscosity or as the vortex viscosity, σ – the microrotation component normal to the xy-plane, $\upsilon_s = (\mu + S/2)j$ is the microrotation viscosity or spin-gradient viscosity, j – the micro-inertia per unit mass, T – the temperature of the fluid within the boundary layer, T_∞ – the temperature of the fluid outside the boundary layer, U_∞ – the velocity of the fluid far away from the plate, c_p – the specific heat of the fluid at constant pressure, κ – the thermal conductivity of the fluid, Q_0 – the heat generation parameter, g_0 – the acceleration due to gravity, and β^* – the volumetric coefficient of thermal expansion. In the present work we assume that the micro-inertia per unit mass j is constant.

The appropriate boundary conditions

- on the plate surface ($y = 0$):

$$u = 0,\ v = v_0(x) \text{ (no-slip and permeable wall conditions)} \tag{5a}$$

$$\sigma \quad n\frac{\partial u}{\partial y} \text{ (microrotation proportional to vorticity), and} \tag{5a}$$

$$\kappa \ \frac{\partial T}{\partial y} \quad q_w \text{ (uniform surface heat flux),} \tag{5a}$$

- matching with the quiescent free stream ($y \quad \infty$):

$$u = U_\infty, \quad \sigma = 0, \quad T = T_\infty \tag{5b}$$

where the subscripts w and ∞ refer to the wall and boundary layer edge, respectively. Positive and negative values of v_0 indicate blowing and suction, respectively, while $v_0 = 0$ corresponds to an impermeable plate. A linear relationship between microrotation function σ and the surface shear $u/\ y$ is chosen for investigating the effect of different surface conditions for microrotation. When microrotation parameter $n = 0$ we obtain $\sigma = 0$ which is a generalization of the no-slip condition *i. e.* the microelements in a concentrated particle flow closest to the wall are not able to translate or rotate as stated by Jena *et al.* [18]. The case $n \quad 0$ states that microrotation is equal to the fluid vorticity at the boundary that is in the neighborhood of a rigid boundary, the effect of microstructure is negligible since the suspended particles can not get closer to the boundary than their radius. Specifically the case $n = 0.5$ represents vanishing of the anti-symmetric part of the stress tensor and represents weak concentration. For this case Ahmadi [5] suggested that in a fine particle suspension the particle spin is equal to the fluid velocity at the wall. The case corresponding to $n = 1$ be representative of turbulent boundary layer flows (see [19]. In eq. (5a), the last condition represents uniform heat flux at the surface of the plate.

Transformation of model

A stream function ψ defined by $u = \ \psi/\ y$ and $v = - \ \psi/\ x$ is introduced such that the continuity eq. (1) is satisfied. To obtain solutions, the governing eqs. (1)-(4) and boundary conditions (5) are first transformed into locally self-similar form because similar solution is more convenient to study. To do this, we now introduce the following transformations:

$$\psi \quad \sqrt{2\upsilon U_\infty x}\,\mathrm{f}(\eta), \quad \sigma \quad \sqrt{\frac{U_\infty^3}{2\upsilon x}}g, \quad \eta \quad y\sqrt{\frac{U_\infty}{2\upsilon x}} \tag{6}$$

Since $u = \ \psi/\ y$ and $v = - \ \psi/\ x$ we have from eq. (6) that, $u = U_\infty f'$ and

$$v \quad \sqrt{\frac{\upsilon U_\infty}{2x}}(f \quad \eta f \ ) \tag{7}$$

Here f is the non-dimensional stream function, g – the dimensionless microrotation, and η – the similarity variable and prime denotes differentiation with respect to η.

The thermal boundary conditions depend on the type of heating process being considered, that is the prescribed heat flux. Define the temperature distribution as follows:

$$T - T_\infty = \theta(\eta)T^* \tag{8}$$

where $T^* = (2\upsilon x/U_\infty)^{1/2} q_\mathrm{w}/\kappa$.

Now substituting eqs. (6)-(8) into eqs. (2)-(4) we obtain:

$$(1 \quad \Delta)f \qquad ff \qquad \Delta g \qquad \lambda\theta \quad 0 \tag{9}$$

$$1 \quad \frac{1}{2}\Delta \quad \xi g \qquad 2\Delta(2g \quad f \ ) \quad \xi(fg \quad gf) \quad 0 \tag{10}$$

$$\theta \qquad \Pr(f\theta \qquad f\ \theta) \quad \Pr Q\theta \quad 0 \tag{11}$$

where $\Delta = S/\mu$ is the vortex viscosity parameter, $\lambda = 2g_0\beta^* x T^*/U_\infty^2$ – the buoyancy parameter, $\xi = jU_\infty/\upsilon x$ – the micro-inertia density parameter, $\Pr = \kappa/\rho c_\mathrm{p}$ – the Prandtl number, and $Q = 2Q_0 x/\rho c_\mathrm{p} U_\infty$ – the non-dimensional heat generation parameter.

The corresponding boundary conditions (5) become:

$$\begin{array}{llll} f \quad f_\mathrm{w}, & f \quad 0, & g \quad nf \ , & \theta \quad 1 \quad \text{at } \eta \quad 0 \\ f \quad 1, & g \quad 0, & \theta \quad 0 & \qquad\quad \text{as } \eta \quad \infty \end{array} \tag{12}$$

where $f_\mathrm{w} = - v_0(x)(2x/\upsilon U_\infty)^{1/2}$ is the suction velocity at the plate for $f_\mathrm{w} > 0$.The eqs. (9)-(11) are locally self similar together with the boundary conditions (12).

Skin friction coefficient, plate couple stress, and Nusselt number

The quantities of chief physical interest are the skin friction coefficient, plate couple stress and the Nusselt number (rate of heat transfer). The equation defining the wall shear stress is:

$$\tau_\mathrm{w} \quad (\mu \quad S)\left.\frac{\partial u}{\partial y}\right|_{y \ 0} \qquad S(\sigma)_{y \ 0} \tag{13}$$

The local skin friction coefficient is defined as:

$$C_f \quad \frac{\tau_\mathrm{w}}{\frac{1}{2}\rho U_\infty^2} \quad \sqrt{2}\frac{1}{\sqrt{\mathrm{Re}_\mathrm{x}}}[1 \quad (1 \quad n)\Delta]f \ (0) \tag{14}$$

Thus from eq. (14) we see that the local values of the skin friction coefficient C_f is proportional to $f \ (0)$.

The equation defying the plate couple stress is:

$$M_\mathrm{w} \quad \mu \quad \frac{S}{2} \ j \left.\frac{\partial\sigma}{\partial y}\right|_{y \ 0} \tag{15}$$

The dimensionless couple stress is defined by:

$$M_{\mathrm{x}} \quad \frac{M_{\mathrm{w}}}{\frac{1}{2}\rho\upsilon U_{\infty}} \quad 1 \quad \frac{1}{2}\Delta \quad \xi g\ (0) \tag{16}$$

Thus the local couple stress in the boundary layer is proportional to $g'(0)$

We may define a non-dimensional coefficient of heat transfer, which is known as Nusselt number as follows:

$$\mathrm{Nu}_{\mathrm{x}} \quad \frac{xh(x)}{\kappa} \tag{17}$$

where $h(x) = q_{\mathrm{w}}/(T_{\mathrm{w}} - T_{\infty})$ and q_{w} is the quantity of heat transferred through the unit area of the surface. Now the rate of heat transfer, in terms of the dimensionless Nusselt number, given by:

$$\mathrm{Nu}_{\mathrm{x}} \quad \sqrt{\mathrm{Re}_{\mathrm{x}}}\,\frac{1}{\sqrt{2}\theta(0)} \tag{18}$$

Thus from eq. (18) we see that the local Nusselt number Nu_{x} is proportional to $1/\theta(0)$. Hence the numerical values corresponding to $C_{\mathrm{f}}\,\mathrm{Re}_{\mathrm{x}}^{1/2}$, M_{x}, and $\mathrm{Nu}_{\mathrm{x}}\mathrm{Re}_{\mathrm{x}}^{\;1/2}$ are calculated from eqs. (14), (16), and (18) are shown in figs. (5)-(7).

Numerical solution

The set of eqs. (9)-(11) are highly non-linear and therefore the system cannot be solved analytically. The non-linear ordinary differential eqs. (9)-(11) with boundary conditions (12) are solved using Nachtsheim-Swigert [20] shooting iteration technique with f_{w}, Δ, Q, ξ, λ, Pr, and n as prescribed parameters. For a brief discussion of the Nachtsheim-Swigert shooting iteration technique authors are suggested to consult the work of Maleque *et al.* [21]. Within the context of the initial value method and the Nachtsheim-Swigert shooting iteration technique the outer boundary conditions may be functionally represented by the first order Taylor's series as:

$$f\ (\eta_{\max}) \quad f\ (\alpha,\beta,\gamma) \quad f_0(\eta_{\max}) \quad \Delta\alpha f_\alpha \quad \Delta\beta f_\beta \quad \Delta\gamma f_\gamma \quad \delta_1 \tag{19}$$

$$g(\eta_{\max}) \quad g(\alpha,\beta,\gamma) \quad g_0(\eta_{\max}) \quad \Delta\alpha g_\alpha \quad \Delta\beta g_\beta \quad \Delta\gamma g_\gamma \quad \delta_2 \tag{20}$$

$$\theta(\eta_{\max}) \quad \theta(\alpha,\beta,\gamma) \quad \theta_0(\eta_{\max}) \quad \Delta\alpha\theta_\alpha \quad \Delta\beta\theta_\beta \quad \Delta\gamma\theta_\gamma \quad \delta_3 \tag{21}$$

with the asymptotic convergence criteria given by:

$$f\ \ (\eta_{\max}) \quad f\ \ (\alpha,\beta,\gamma) \quad f_0(\eta_{\max}) \quad \Delta\alpha f_\alpha \quad \Delta\beta f_\beta \quad \Delta\gamma f_\gamma \quad \delta_4 \tag{22}$$

$$g\ (\eta_{\max}) \quad g\ (\alpha,\beta,\gamma) \quad g_0(\eta_{\max}) \quad \Delta\alpha g_\alpha \quad \Delta\beta g_\beta \quad \Delta\gamma g_\gamma \quad \delta_5 \tag{23}$$

$$\theta\ (\eta_{\max}) \quad \theta\ (\alpha,\beta,\gamma) \quad \theta_0(\eta_{\max}) \quad \Delta\alpha\theta_\alpha \quad \Delta\beta\theta_\beta \quad \Delta\gamma\theta_\gamma \quad \delta_6 \tag{24}$$

where $\alpha = f''(0)$, $\beta = g'(0)$, $\gamma = \theta(0)$, and α, β, and γ subscripts indicate partial differentiation, *e. g.*, $f_\alpha = f'/f''(0)$. The subscript 0 indicates the value of the function at $\eta_{\max}$ to be determined from the trial integration. Solution of these equations in a least-squares sense requires determining the minimum value of $E = (\delta_1 - 1)^2 + \delta_2^2 \quad \delta_3^2 \quad \delta_4^2 \quad \delta_5^2 \quad \delta_6^2$ with respect to α, β, and γ. To solve $\Delta\alpha, \Delta\beta$, and $\Delta\gamma$ we require to differentiate E with respect to α, β, and γ, respectively. Thus adopting this numerical technique, a computer program was set up for the solutions of the governing non-linear partial differential equations of our problem where the integration technique was adopted as a sixth-order Runge-Kutta method of integration.

A step size of $\Delta\eta = 0.001$ was selected to be satisfactory for a convergence criterion of 10^{-6} in all cases. The value of η_∞ was found to each iteration loop by the statement $\eta_\infty = \eta_\infty + \Delta\eta_\infty$. The maximum value of η_∞, to each group of parameters f_w, Δ, Q, ξ, λ, Pr, and n is determined when the value of the unknown boundary conditions at $\eta = 0$ not change to successful loop with error less than 10^{-6}.

In order to verify the effects of the step size $\Delta\eta$ we ran the code for our model with three different step sizes as, $\Delta\eta = 0.01$, $\Delta\eta = 0.005$, and $\Delta\eta = 0.001$ and in each case we found excellent agreement among them. Figures 2a-c, respectively, show the velocity, microrotation, and temperature profiles for different step sizes. From these figures it is clear that for sufficiently small values of $\Delta\eta$ the solutions are independent of the step sizes.

To assess the accuracy of our code, we reproduced the values of $f''(0)$, $g'(0)$, and $-\theta'(0)$, which are proportional, respectively, to the local skin friction coefficient, plate couple stress, and the rate of heat transfer coefficient considering the model of El-Arabawy [22] for Pr = 0.73 and $N = 5.0$ (vhere N is the radiation parameter defined in [22]). Tables 1-3 show the comparison of the data produced by our code and that of El-Arabawy. In fact the results show a close agreement, hence an encouragement for the use of the present code for our model.

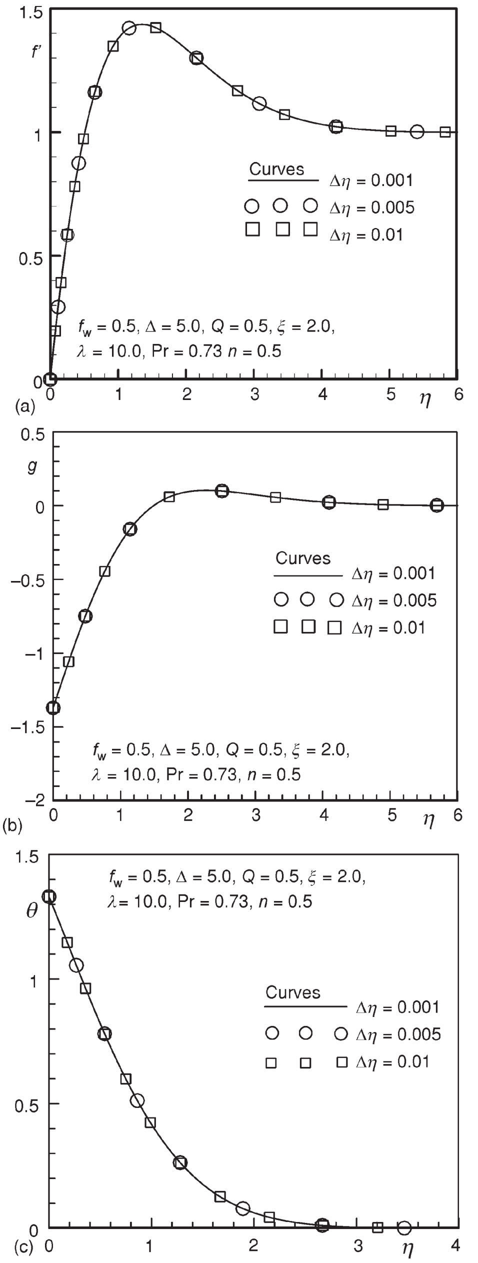

Figure 2. (a) velocity, (b) microrotation, and (c) temperature profiles for different values of $\Delta\eta$

Results and discussion

The present work generalized the problem of heating effects on a boundary layer of a micropolar fluid over the porous plate with variable suction, uniform surface heat flux in the presence of heat generation. For the purpose of discussing the results, the numerical calculations are presented in the form of non-dimensional velocity, microrotation, and temperature profiles. In the calculations the values of suction parameter f_w, vortex viscosity parameter Δ, heat generation parameter Q, micro-inertia density parameter ξ, buoyancy parameter λ, Prandtl number Pr, and microrotation parameter n are chosen arbitrarily.

Table 1. Comparison of $f''(0)$

v_0	Code El-Arabawy [22]	Present code
–0.7	–0.278827	–0.278390
–0.4	–0.404227	–0.403525
–0.2	–0.504059	–0.503800
0.0	–0.616542	–0.616237
0.2	–0.741521	–0.741131
0.4	–0.877517	–0.877088
0.7	–1.099430	–1.098857

Table 2. Comparison of $g'(0)$

v_0	Code El-Arabawy [22]	Present code
–0.7	0.236917	0.236511
–0.4	0.286997	0.286460
–0.2	0.321165	0.320745
0.0	0.355330	0.355138
0.2	0.389278	0.389055
0.4	0.422223	0.421998
0.7	0.468923	0.468660

Table 3. Comparison of $-\theta'(0)$

v_0	Code El-Arabawy [22]	Present code
–0.7	0.247513	0.242280
–0.4	0.316706	0.313005
–0.2	0.370236	0.367887
0.0	0.427013	0.429061
0.2	0.492675	0.496532
0.4	0.565067	0.569655
0.7	0.686869	0.689726

The existence of the free convection current is due to the difference in temperature of the plate T_w and the temperature in the uniform flow, viz. $T_w - T_\infty$. Hence the difference may be positive, zero, or negative depending upon $T_w > T_\infty$. Then the values of λ will assume positive, zero, or negative values. Physically $\lambda < 0$ corresponds to an externally heated plate as the free convection currents are carried towards the plate and $\lambda > 0$ corresponds to an externally cooled plate while corresponds to the absence of free convection currents. Since we are considering cooling problem, only positive values of λ are chosen. The default values of the above-mentioned parameters which we considered are $f_w = 0.5$, $\Delta = 5.0$, $Q = 0.5$, $\xi = 0.5$, $\lambda = 10.0$, $\Pr = 0.73$, and $n = 0.5$ unless otherwise specified.

Figure 3a shows the velocity profiles for different values of suction parameter f_w for a cooling plate. It can be seen that for cooling of the plate the velocity profiles decrease monotonically with the increase of suction parameter. When suction applies, the eventual state of the boundary layer is of uniform thickness indicating suction stabilizes the boundary layer growth. The free convection effect is also apparent in this figure. For a fixed suction velocity f_w, velocity is found to increase and reaches a maximum value in a region close to the plate, then gradually decreases to one. Figure 3b shows the microrotation (angular velocity) profiles for different values of suction parameter. The angular velocity g remains negative for large values of f_w whereas it has a tendency to become positive for small values of f_w. In general, the angular velocity of the microelements increases with the increase of f_w very close to the surface of the plate. As suction velocity intensifies the microrotation of the microconstituents gets induced near the surface of the plate. After a short distance from the surface of the plate (η 1) where kinematic viscosity is dominant these profiles overlap and then decrease with the increase of f_w. Within the boundary layer region these profiles increase from $-0.5 f''(0)$ to zero as η increases from zero to infinity. Figure 3c indicates the temperature profiles showing the effect of suction parameter. It can be seen that temperature decreases with the increase of the suction parameter. Decelerated fluid particles close to the heated wall absorb more heat from the plate as a consequence the temperature of the fluid within the boundary layer increases. Sucking these decelerated fluid particles through the porous plate leads to the decrease of the temperature profiles.

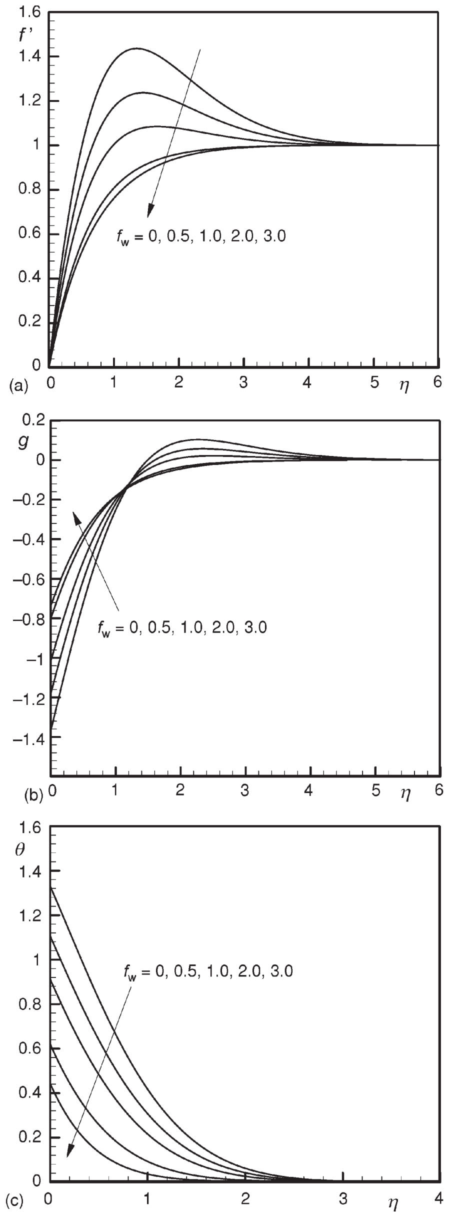

Figure 3. (a) velocity, (b) microrotation, and (c) temperature profiles for different values of suction parameter f_w

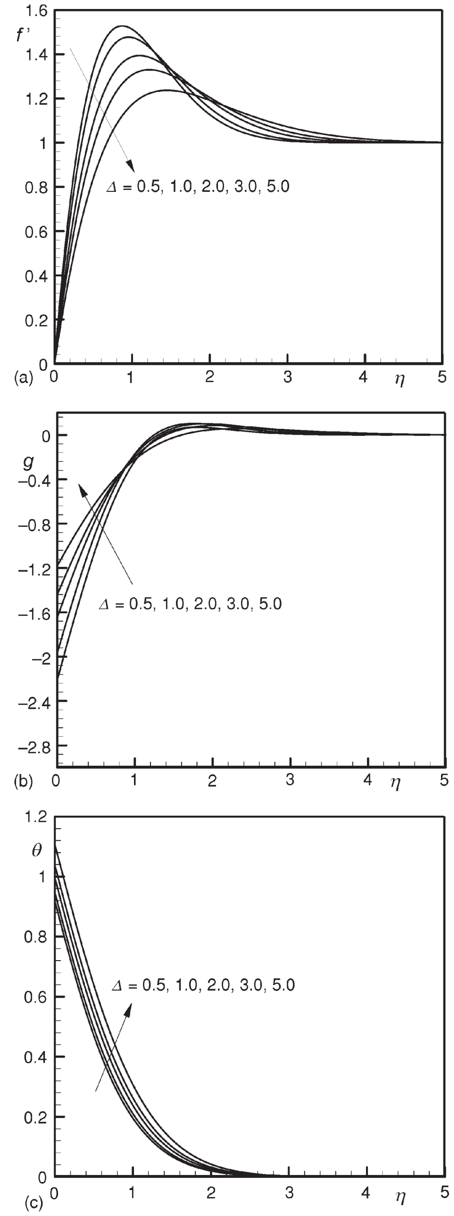

Figure 4. (a) velocity, (b) microrotation, and (c) temperature profiles for different values of vortex viscosity parameter Δ

Thus suction can be used for controlling the temperature function, which is required in many engineering applications like nuclear reactors, generators, *etc*.

Figure 4 a shows the effect of vortex viscosity parameter Δ on the velocity profiles for a cooling plate. From here we see that, as Δ increases, the maximum of the velocity decreases and the location of the maximum velocity increases and shifts away from the surface of the plate. Increasing Δ intensifies the concentration of the microconstituents near the boundary as a consequence the velocity of the micropolar fluid decreases and the thickness of the momentum boundary layer increases. Figure 4b shows the effect of Δ on the microrotation profiles. From this figure we see that microrotation increases with the increase of the vortex viscosity parameter. It is also understood that as the vortex viscosity increases the rotation of the microconstituents gets induced near the wall (η 1). Far away from the wall where kinematic viscosity dominates the flow these profiles overlap and decreases with the increase of Δ. From fig. 4c we found increasing effect of Δ on the temperature profiles. This figure also reveals that thermal boundary layer thickness becomes large as Δ is increased.

Figures 5a-5c, respectively, show the velocity, microrotation, and temperature profiles for different values of heat generation parameter Q. From fig. 5a it is observed that when the heat is generated the buoyancy force increases which induces the flow rate to increase giving rise to the increase in the velocity profiles as a consequence the momentum boundary layer thickness decreases. Figure 5b shows the effects of heat generation on the microrotation profiles. The microrotation (angular velocity) is found to decrease as Q increases because Q increases the buoyancy in the vicinity of the plate. But far away from the surface of the plate where buoyancy force is week these profiles increase with the increase of Q. Owing to the presence of heat generation it is apparent that there is an increase in the thermal state of the fluid. Hence from fig. 5c we observe that temperature increases as Q increases. It is also apparent that the thickness of the thermal boundary layer increases with the increase of heat generation.

In figs. 6a-6c, respectively, we have varied the micro-inertia density parameter ξ keeping all other parameters value fixed. From fig. 6a we see that as ξ increases the inertia of the microconstituents increases as a result velocity of the micropolar fluid decreases very close to the surface of the plate (η 1). Away from the velocity surface fluid velocity increases with the increase of ξ. From fig. 6b we see that microrotation profiles decrease with the increase of micro-inertia density parameter except near the surface of the plate where kinematic viscosity dominates the flow. From fig. 6c we see that the values of ξ introduce negligible increasing effect on the temperature profiles.

In figs. 7a-7c, respectively, we have presented the physical parameters skin friction coefficient

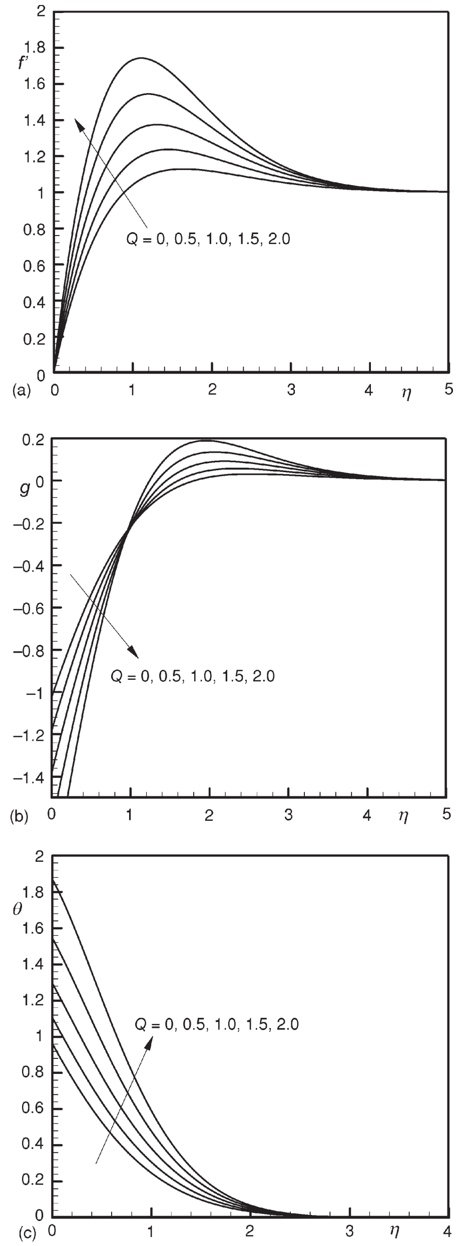

Figure 5. (a) velocity, (b) microrotation, and (c) temperature profiles for different values of heat generation parameter Q

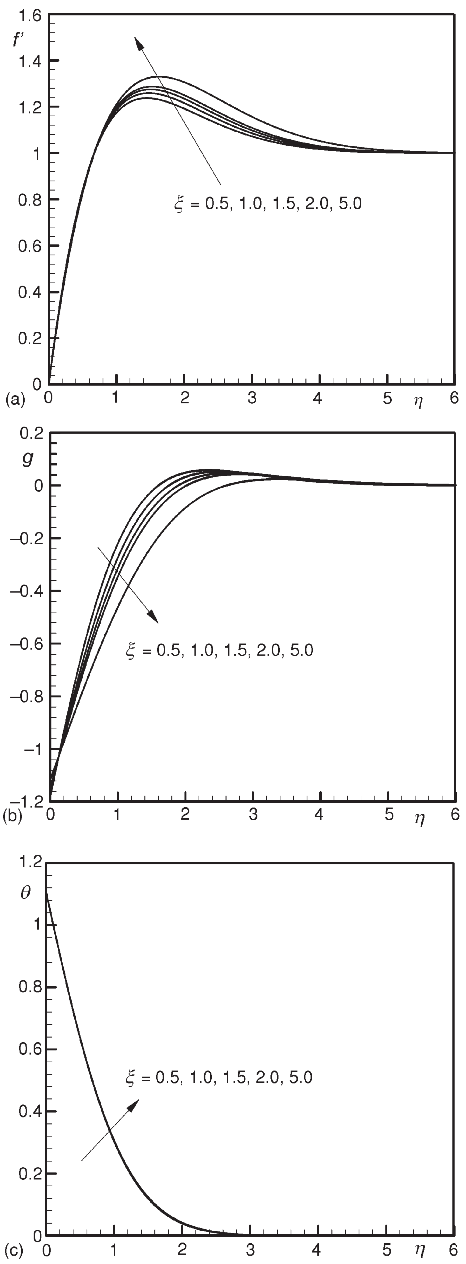

Figure 6. (a) velocity, (b) microrotation, and (c) temperature profiles for different values of micro-inertia density parameter ξ

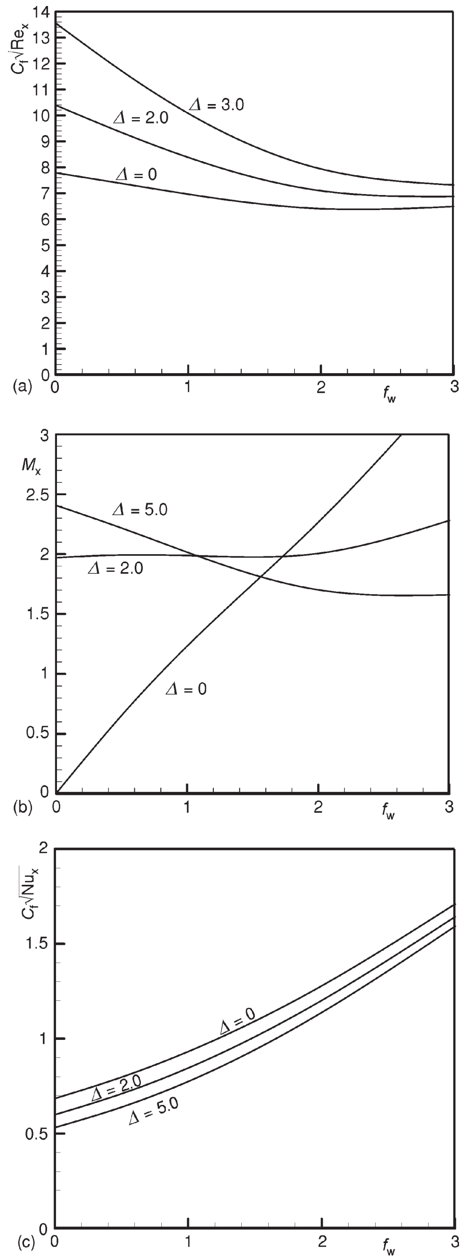

Figure 7. (a) skin friction coefficient, (b) plate couple stress, and (c) Nusselt number for different values of suction parameter f_w and vortex viscosity parameter Δ

(surface shear stress), plate couple stress and the rate of heat transfer (Nusselt number) for different values of suction parameter f_w and vortex viscosity parameter Δ. From fig. 7a we see that skin friction coefficient decreases with the increase of f_w whereas for a fixed value of f_w this coefficient increases with the increase of Δ. As Δ increases the vortex viscosity of the micropolar fluid increases therefore the rate of friction between the fluid and plate increases. It is also apparent that for small suction increasing effect of Δ is significant. Figure 7b shows that for $\Delta < 2.7$ (not precisely determined) plate couple stress increases with the increase of f_w. For Δ 2.7 plate couple stress decreases with the increase of f_w. It is also noticeable that M_x increases with the increase of Δ up to a certain value of f_w then it decreases with the further increase of f_w. From fig. 7c we observe that rate of heat transfer increases with the increase of f_w whereas this coefficient decreases with the increase of Δ.

Figures 8a-8c, respectively, show the skin friction coefficient, plate couple stress, and the rate of heat transfer for different values of heat generation parameter Q, and buoyancy parameter λ. From this figure we see that skin friction coefficient increases with the increase of heat generation parameter for the case of free convection (large λ). In the absence of free convection ($\lambda = 0$) this coefficient remains the same. For a fixed value of Q skin friction increases with the increase of λ. Effects of Q and λ on the plate couple stress are same as those of skin friction coefficient. Figure 8c shows that rate of heat transfer increases with the increase of λ whereas this coefficient decreases with the increase of Q. The heat generation mechanism increases the fluid temperature near the surface of the plate as a consequence rate of heat transfer from the plate to the fluid decreases. The buoyancy parameter as well as heat generation parameter has thus an important role in controlling the temperature.

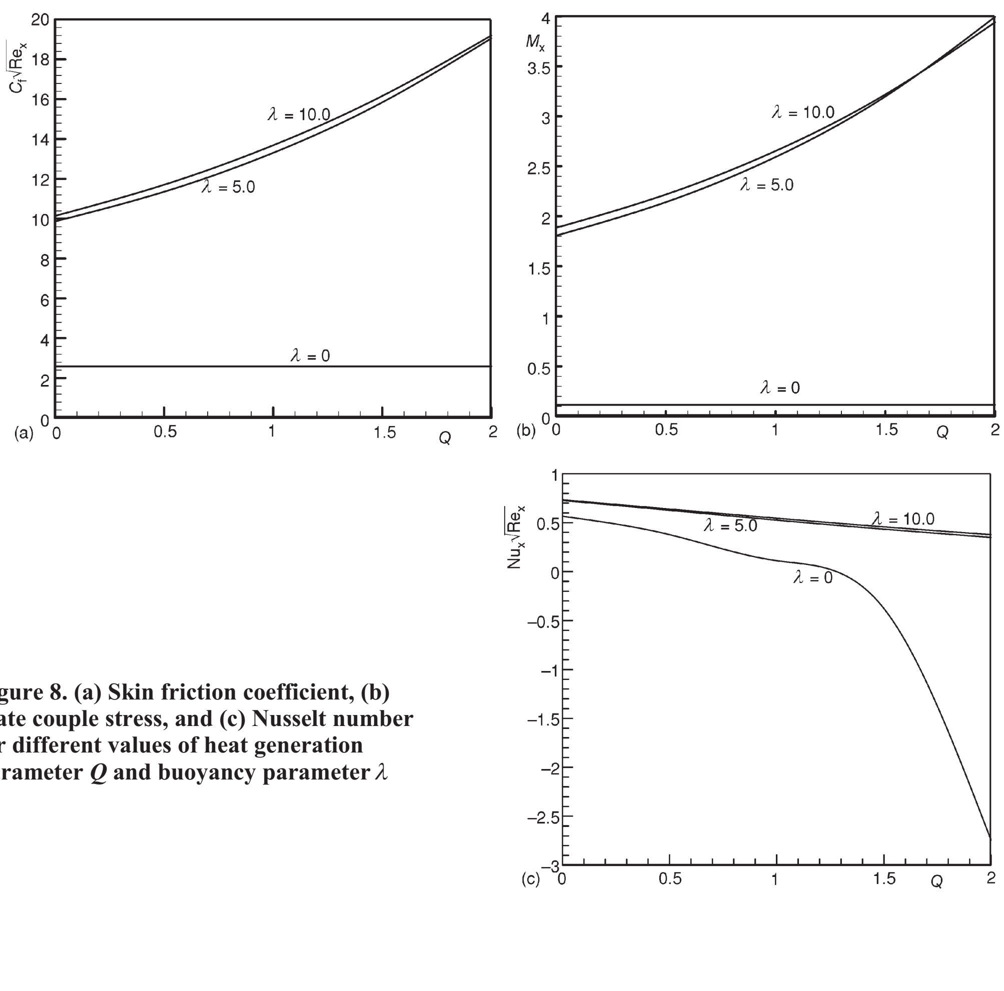

Figure 8. (a) Skin friction coefficient, (b) plate couple stress, and (c) Nusselt number for different values of heat generation parameter Q and buoyancy parameter λ

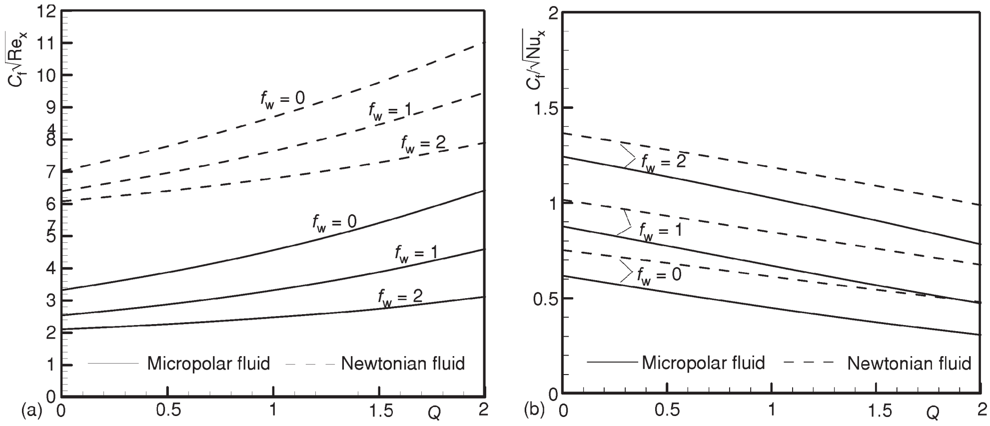

Figure 9. (a) skin friction, and (b) Nusselt number in micropolar fluid and Newtonian fluid for different values of suction parameter f_w and heat generation parameter Q

Figures 9a and 9b, respectively, show the skin friction coefficient and rate of heat transfer for different values of f_w and Q in a micropolar fluid (solid line) and a Newtonian fluid (dashed line). In our problem $\Delta = 0$ and $\xi = 0$ represents the case of a Newtonian fluid. From these figures we observe that skin friction coefficient as well as rate of heat transfer is lower in the micropolar fluid compared to the Newtonian fluid, which may be beneficial in flow and temperature control of polymer processing.

Conclusions

In this paper, we have investigated numerically the heat transfer flow of thermo-micropolar fluid past a vertical permeable flat plat with uniform surface heat flux in the presence of heat generation. Using usual similarity transformations the governing equations have been transformed into non-linear coupled ordinary differential equations and were solved for similar solutions by using Nachtsheim-Swigert shooting iteration technique. Effects of the various parameters such as suction parameter f_w, vortex viscosity parameter Δ, heat generation parameter Q, micro-inertia density parameter ξ, and buoyancy parameter λ on the flow, microrotation, and temperature profiles are examined. The following conclusions can be drawn as a result of the numerical computations.

Skin friction (surface shear stress) coefficient decreases with the increase of suction parameter and vortex viscosity parameter, indicating that these parameters accelerate the flow regime. Thus drag forces can be reduced by an increase in the suction parameter and vortex viscosity parameter. Skin friction coefficient increases with the increase of the buoyancy parameter and heat generation parameter.

Plate couple stress increases with the increase of suction parameter for $\Delta < 2.7$, vortex viscosity parameter for small suction, buoyancy parameter, and heat generation parameter.

The rate of heat transfer increases with the increase of the suction parameter and buoyancy parameter. This coefficient decreases with the increase of the vortex viscosity parameter and heat generation parameter. The increase in heat transfer rate indicates a fast cooling of the plate.

The skin friction coefficient as well as rate of heat transfer is lower in the micropolar fluid compared to that of the Newtonian fluid.

Nomeclature

C_f – local skin-friction coefficient $(= 2\tau_w/\rho U_\infty^2)$, [–]
c_p – specific heat due to constant pressure, [$Jkg^{-1}K^{-1}$]
f – dimensionless stream function, [–]
f_w – dimensionless wall suction, [–]
g – dimensionless microrotation, [–]
g_0 – acceleration due to gravity, [ms^{-2}]
j – micro-inertia per unit mass, [m^2]
M_w – plate couple stress, [Pa·m]
Nu_x – local Nusselt number $(= xh(x)/\kappa)$, [–]
n – microrotation parameter, [–]
Pr – Prandtl number $(= \mu c_p/\kappa)$, [–]
Q – dimensionless heat generation parameter, $(= 2Q_0x/\rho c_p U_\infty)$, [–]
Q_0 – heat generation parameter, [W]
q_w – surface heat flux, [Wm^{-2}]
S – coefficient of vortex viscosity, [Pa·s]
T – temperature of the fluid within the boundary layer, [K]
T_w – temperature at the surface of plate, [K]
T_∞ – temperature of the ambient fluid, [K]
U_∞ – free stream velocity, [ms^{-1}]
u, v – the x and y component of the velocity – field, [ms^{-1}]
$v_0(x)$ – transpiration velocity, [ms^{-1}]
x, y – axis in direction along and normal to the plate [m]

Greeks letters

β^* – volumetric coefficient of thermal expansion, [K^{-1}]
Δ – vortex viscosity parameter $(= S/\mu)$, [–]
θ – dimensionless temperature $(T - T_\infty/T^*)$, [–]
κ – thermal conductivity of fluid, [$Wm^{-1}K^{-1}$]
λ – local bouyancy parameter $(= 2g_0\beta^* xT^*/U_\infty^2)$, [–]
μ – fluid viscosity, [Pa·s]
ξ – micro-inertia density parameter
ρ – fluid density, [kgm^{-3}]
σ – microrotation component normal – to xy plane, [s^{-1}]
τ_w – wall shear stress, [Pa]
υ – kinematic viscosity, [m^2s^{-1}]
ψ – stream function, [m^2s^{-1}]

Subscripts

w – surface conditions
∞ – conditions far away from the surface

References

[1] Eringen, A. C., Theory of Micropolar Fluids, *J. Math. Mech., 16* (1966), 1, pp.1-18
[2] Hadimoto, B., Tokioka, T., Two-Dimensional Shear Flows of Linear Micropolar Fluids, *Int. J. Eng. Sci., 7* (1969), 5, pp. 515-522
[3] Lockwood, F., Benchaitra, M., Friberg, S., Study of Lyotropic Liquid Crystals in Viscometric Flow and Clastohydrodynamic Contact, *ASLE Tribology Trans., 30* (1987), 4, pp. 539-548
[4] Ariman, T., Turk, M. A., Sylvester, N. D., Microcontinuum Fluid Mechanics – A Review, *Int. J. Eng. Sci., 12* (1974), 4, pp. 273-293
[5] Ahmadi, G., Self-Similar Solution of Incompressible Micropolar Boundary Layer Flow over a Semi- Infinite Plate, *Int. J. Eng. Sci., 14* (1976), 7, pp. 639-646
[6] Soundalgekar, V. M., Takhar, H. S., Flow of a Micropolar Fluid on a Continuous Moving Plate, *Int. J. Eng. Sci., 21* (1983), 8, pp. 961-965
[7] Gorla, R. S. R., Mixed Convection in a Micropolar Fluid from a Vertical Surface with Uniform Heat Flux, *Int. J. Engng. Sci., 30* (1992), 3, pp. 349-358
[8] Rees, D. A. S., Pop, I., Free Convection Boundary Layer Flow of Micropolar Fluid from a Vertical Flat Plat, *IMA J. Appl. Math., 61* (1998), 2, pp. 179-197
[9] Mohammadein, A. A., Gorla, R. S. R., Heat Transfer in a Micropolar Fluid over a Stretching Sheet with Viscous Dissipation and Internal Heat Generation, *Int. J. Num. Meth., Heat Fluid Flow., 11* (2001), 1, pp. 50-58
[10] Aissa, W. A., Mohammadein, A. A., Joule Heating Effects in a Micropolar Fluid Past a Stretching Sheet with Variable Electric Conductivity, *J. Comput. Appl. Mech., 6* (2005), 1, pp. 3-13
[11] Markin, J. H., Mahmood,T., Mixed Convection Boundary Layer Similarity Solution, Prescribed Heat Flux, *ZAMP., 40* (1989), 1, pp. 61-68
[12] Char, M.-I., Chang, C.-L., Laminar Free Convection Flow of Micropolar Fluids from a Curved Surface, *J. Phys. D: Appl. Phys., 28* (1995), 7, pp. 1324-1331

[13] Kelson, N. A., Farrell, T. W., Micropolar Flow over a Porous Stretching Sheet with Strong Suction or Injection, *Int. Comm. Heat Mass Transfer., 28* (2001), 4, pp. 479-488
[14] Bhargava, R., Kumar, L., Takhar, H. S., Finite Element Solution of Mixed Convection Micropolar Flow Driven by a Porous Stretching Sheet, *Int. J. Engng. Sci., 41* (2003), 18, pp. 2161-2178
[15] Bhargava, R., *et al.*, Numerical Solutions for Micropolar Transport Phenomena over a Nonlinear Stretching Sheet, *Nonlin. Analy.: Modl. Control., 12* (2007), 1, pp. 45-63
[16] Rahman, M. M., Sattar, M. A., Magneto Hydrodynamic Convective Flow of a Micropolar Fluid Past a Continuously Moving Vertical Porous Plate in the Presence of Heat Generation/Absorption, *ASME J. H. Transfer., 128* (2006), 2, pp. 142-152
[17] Rahman, M. M., Sultana, T., Radiative Heat Transfer Flow of Micropolar Fluid with Variable Heat Flux in a Porous Medium., *Nonlinear Analysis: Modeling Control, 13* (2008), 1, pp. 71-87
[18] Jena, S. K., Mathur, M. N., Similarity Solution for Laminar Free Convection Flow of Thermo-Micropolar Fluid Past a Non-Isothermal Vertical Flat Plate, *Int. J. Engng. Sci., 19* (1981), 11, pp. 1431-1439
[19] Peddison, J., McNitt, R. P., Boundary Layer Theory for Micropolar Fluid, *Recent Adv. Eng. Sci., 5* (1970), pp. 405-426
[20] Nachtsheim, P. R., Swigert, P., Satisfaction of the Asymptotic Boundary Conditions in Numerical Solution of the System of Non-Linear Equations of Boundary Layer Type, NASA TND-3004, 1965
[21] Maleque, K. A., Sattar, M. A., The Effects of Variable Properties and Hall Current on Steady MHD Laminar Convective Fluid Flow Due to a Porous Rotating Disk, *Int. J. Heat Mass Trans., 48* (2005), 23-24, pp. 4963-7492
[22] El-Arabawy, H. A. M., Effect of Suction/Injection on the Flow of a Micropolar Fluid Past a Continuously Moving Plate in the Presence of Radiation, *Int. J. Heat Mass Transfer., 46* (2003), 8, pp. 1471-1477

Authors' affiliation:

M. M. Rahman (**corresponding author**)
Department of Mathematics and Statistics,
College of Science, Sultan Qaboos University
P.O. Box 36, Al-Khod 123, Muscat, Sultanate of Oman
E-mail: mansurdu@yahoo.com

I. A. Eltayeb
Department of Mathematics and Statistics
College of Science, Sultan Qaboos University
Sultanate of Oman

S. M. Mujibur Rahman
Department of Physics, College of Science,
Sultan Qaboos University
Sultanate of Oman

Paper submitted: June 10, 2008
Paper revised: September 9, 2008
Paper accepted: December 8, 2008